Interaction of novel cationic *meso*-tetraphenylporphyrins in the ground and excited states with DNA and nucleotides

Pavel Kubát,*[ab] Kamil Lang,[c] Pavel Anzenbacher Jr.,†[d] Karolina Jursíková,[d] Vladimír Král[d] and Benjamin Ehrenberg[b]

[a] *Institute of Physical Chemistry, Academy of Sciences of the Czech Republic, Dolejškova 3, 182 23 Praha 8, Czech Republic. Fax: +420 2 859 08 25; E-mail: kubat@jh-inst.cas.cz*
[b] *Department of Physics, Bar Ilan University, 52 900 Ramat Gan, Israel*
[c] *Institute of Inorganic Chemistry, Academy of Sciences of the Czech Republic, 250 68 Řež, Czech Republic*
[d] *Prague Institute of Chemical Technology, Technická 5, 166 28 Praha 6, Czech Republic*

Received (in Cambridge, UK) 30th November 1999, Accepted 2nd February 2000

The syntheses and aggregation properties of novel cationic *meso*-tetraphenylporphyrins substituted in the *para*-positions with -CH_2(pyridinio)$^+$ (**P_1**), -$CH_2N^+(CH_3)_3$ (**P_2**), -CH_2P^+(*n*-butyl)$_3$ (**P_3**), -CH_2P^+(phenyl)$_3$ (**P_4**), -$CH_2S^+(CH_3)_2$ (**P_5**) and -$CH_2SC(NH_2)_2^+$ (**P_6**) groups are described. Their use as photosensitizers and their interactions with DNA and nucleotides were studied by optical methods and their properties were compared with those of anionic *meso*-tetrakis(4-sulfonatophenyl)porphyrin (TPPS) and cationic *meso*-tetrakis(4-*N*-methylpyridyl)porphyrin (TMPyP). **P_1** and **P_2** formed stable complexes with calf thymus DNA in phosphate buffer ($K_a \sim 10^6$ M^{-1}; outside stacking binding mode) and with some nucleotides in methanol ($K_a \sim 10^3$–10^4 M^{-1}). **P_3**–**P_6** aggregated readily in aqueous solution due to their more hydrophobic nature. The cationic porphyrins TMPyP and **P_1**–**P_6** sensitized the decomposition of guanosine 5′-monophosphate (GMP). The rates of GMP decomposition were found to be greater with cationic porphyrins **P_1**–**P_6** than with anionic TPPS, presumably because of Coulombic attraction between the positively charged porphyrins **P_1**–**P_6** and the anionic GMP. In oxygen-free conditions, GMP decomposition was initiated by interaction of the singlet (**P_1**, **P_2**) or triplet (**P_1**–**P_6**) excited states of the porphyrins with GMP. In the presence of oxygen, GMP is decomposed predominantly *via* singlet oxygen mechanism.

Introduction

Positively charged porphyrins have attracted considerable attention since their first reported syntheses almost three decades ago[1,2] chiefly because of their remarkable ability to form complexes with and cleave nucleic acids, a property described in pioneer works by Fiel *et al*.[3] Since the molecular recognition of DNA is of fundamental importance to life, analyzing the interaction of small molecules with DNA continues to be an important area of research. Within the context of this general theme, the binding of cationic porphyrins to DNA is of considerable interest. Potential applications of these systems include photodynamic therapy of cancer (PDT),[4] molecular biology applications such as DNA footprinting,[5] design of telomerase inhibitors,[6] stabilizing DNA/RNA hybrids,[7] DNA triplexes[8] or quadruplexes,[9] specific sensing of DNA quadruplexes,[10] antiviral agent development,[11] and the development of materials for selective cleavage of DNA[12] and RNA.[13] Porphyrin and/or metalloporphyrin mediated cleavage of nucleic acids occurs *via* oxidative attack on the sugar moiety,[14] nucleobase modifications which lead to strand scission,[15] or by a photoinduced mechanism involving either the porphyrin excited state or singlet oxygen.[16] Further, porphyrin-induced changes of DNA conformation could allow for the specific probing of DNA structure.[17] Not surprisingly, developments in this area are predicated upon a detailed understanding of the porphyrin–nucleic acid binding mechanism.

Despite the extensive studies devoted to the pyridinium and ammonium porphyrins,[1,2] very few other types of positively charged tetraarylporphyrins have been prepared. These include the α-trialkylammonium tetratolylporphyrins of Robic *et al.*[18] and Jin *et al*.,[19] the guanidinium porphyrin of Salehi *et al*.[20] and the α-trialkyl- and α-triaryl-phosphonium tetratolylporphyrins prepared independently by our group[21] and by Jin *et al.*[22] Unfortunately, none of these porphyrins have been studied under similar conditions, so properties cannot be easily compared.

Three generalized binding models have been described for the interaction of cationic porphyrins with DNA: i) intercalation, ii) outside groove binding and iii) outside binding with self-stacking, a mode that leads to the production of organized porphyrin structures on the DNA exterior.[3,23–25] Intercalative binding of free-base *meso*-tetrakis(4-*N*-methylpyridyl)porphyrin (TMPyP) and corresponding planar metal derivatives leads to a large red shift (>10 nm) and an extensive hypochromicity of the Soret band.[3,23] The Soret region is usually very sensitive to factors such as solvent, concentration, aggregation, ionic strength, binding of small molecules, although the visible (Q) bands are less affected.

The binding of porphyrins, especially those that contain hydrophobic substituents, is often complicated by their aggregation in aqueous solutions. TMPyP, for example, was not found to be aggregated at concentrations lower than 10^{-3} M in aqueous media.[25] On the other hand porphyrins bearing phosphonium residues were strongly aggregated in water, as the result of π–π stacking interactions.[22]

DNA complexes involving porphyrins such as TMPyP are presumably stabilized by electrostatic interactions between the positively charged substituents on the porphyrin periphery and

† *Current address*: University of Texas at Austin, Austin, Texas, 78712-1167, U.S.A.

DOI: 10.1039/a909466k

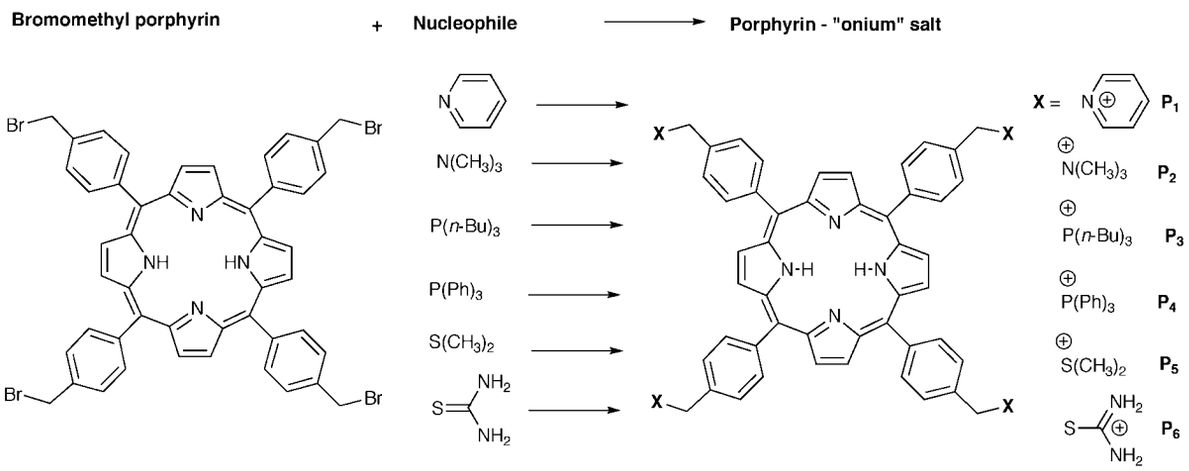

Fig. 1 Structures and general strategy for synthesis of cationic *meso*-tetraphenylporphyrins bearing substituents with positive charge on nitrogen ($\mathbf{P_1}$, $\mathbf{P_2}$, $\mathbf{P_6}$), phosphorus ($\mathbf{P_3}$, $\mathbf{P_4}$) and sulfur ($\mathbf{P_5}$, $\mathbf{P_6}$) atoms.

the negatively charged phosphate oxygen atoms of DNA. When a DNA-bound porphyrin is photoexcited, photosensitized cleavage of DNA and nucleotides can be initiated by electron and/or energy transfer between the excited porphyrin and an adjacent base pair. Because the triplet states of TMPyP bound to DNA exhibit longer lifetimes than those of unbound TMPyP,[26] electron and/or energy transfer events involving the bound porphyrins are more probable. The triplet excited states of porphyrins can be quenched by oxygen, producing singlet oxygen in close proximity to DNA. The "weak link" in the DNA chain is guanine; the rate constants for the reaction of singlet oxygen with guanine ($>10^6$ $M^{-1}s^{-1}$) greatly exceed those of adenine, cytidine and thymine.[27–29]

The particular sensitizers reported here are derivatives of *meso*-tetraphenylporphyrin (TPP), which is itself known to be a good sensitizer with high quantum yield of singlet oxygen (0.34 – 0.87).[30] Any practical use of this compound is precluded by its lack of solubility in water. Here we describe a general synthetic approach for the preparation of tetrasubstituted derivatives of TPP with positively charged ammonium, pyridinium, phosphonium and sulfonium groups. The synthetic strategy is based on the reaction of suitable nucleophiles such as trialkylphosphine, triarylphosphine, alkylarylphosphine, dialkyl sulfide, trialkylamine, pyridine or pyridine-type derivatives with tetrakis(4-bromomethyl)porphyrin.[31,32] The cationic centers are insulated from the porphyrin ring by a methylene bridge and thus have minimal influence on the electron density in the π-system of the porphyrin chromophore. From a design perspective, these porphyrins were expected to display photophysical properties similar to those of TPP, yet be water soluble and exhibit binding affinities for DNA augmented by the charged substituents.

Before studying the photosensitization of cellular systems by the porphyrins $\mathbf{P_1}$–$\mathbf{P_6}$ (Fig. 1), we examined the aggregation properties and basicity of these porphyrins as well as the stability of complexes formed with nucleotides and DNA. Guanosine 5′-monophosphate (GMP) was employed as a model for DNA damage, and results obtained were compared with the behavior of cationic TMPyP and anionic *meso*-tetrakis(4-sulfonatophenyl) porphyrin (TPPS).

Results and discussion

A. Design and synthesis of porphyrins

We have developed a general strategy for easy access to novel positively charged porphyrins. *meso*-Tetrakis(bromo-*p*-tolyl)-porphyrin was prepared following literature procedures[31,32] and then used to quaternize using a variety of nucleophiles including phosphines, sulfide, amine, pyridine and thiourea. This approach has several advantages. First of all it is very versatile and therefore widely applicable to all kinds of tertiary aromatic and aliphatic amines, phosphines, substituted pyridines, substituted thioureas and aliphatic dialkyl sulfides. This generalized approach, summarized in Fig. 1, provides the corresponding positively charged porphyrin-phosphonium, sulfonium, ammonium, isothiouronium derivatives. Porphyrins $\mathbf{P_1}$–$\mathbf{P_6}$ (Fig. 1) are soluble in water, DMSO and methanol. Control of the steric bulk and polar properties of the original nucleophile allows fine tuning of the porphyrin properties to suit possible medical applications. The lipophilic substituents (*e.g.* phenyl, butyl) may make it easier for the porphyrin derivative to pass through or accumulate in biomembranes, thus potentially altering the localization of the porphyrin derivative within the cell compartments. It is therefore conceivable that alkyl or aryl residues at the quaternized site may play an important role in directing photosensitizing ability toward different tissues or cell compartments. These factors provide a compelling driving force for detailed study of the physicochemical properties of $\mathbf{P_1}$–$\mathbf{P_6}$.

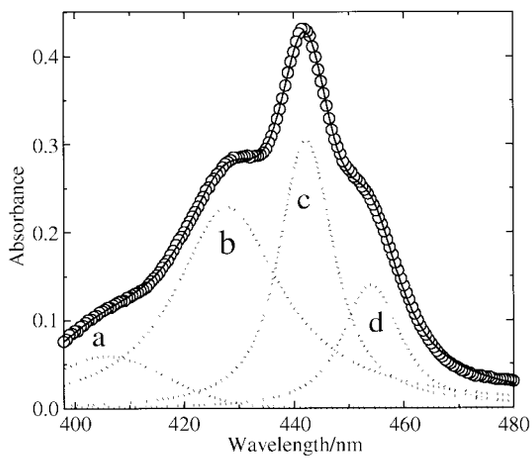

Fig. 2 Soret band of 2.7 μM $\mathbf{P_4}$ in water at pH 3.1. Superposition of four Voigtians resolved in wavenumber units: H-aggregate (a), monomer (b), J-aggregate (c), protonated porphyrin (d).

B. Aggregation and protonation in aqueous solution

The Soret bands of $\mathbf{P_1}$–$\mathbf{P_6}$ comprise four sub-bands. Their relative intensities depend on pH, porphyrin concentration, solution history (*e.g.* degree of aging), and porphyrin functionalization. The shapes of the individual sub-bands were analyzed using a Voigt function[38] (convolution of a Lorenzian function with a Gaussian function) in order to resolve the respective absorption bands (Table 1). A detailed spectral analysis of $\mathbf{P_4}$ at pH 3.1 is shown in Fig. 2 as an example. The

Table 1 Soret band maxima for monomer, aggregates and protonated porphyrins $\mathbf{P_1}$–$\mathbf{P_6}$, TPPS and TMPyP in 20 mM phosphate buffer, pH 7.0. Designation according to Fig. 1

	λ/nm (10^{-5} ε/M^{-1} cm^{-1})			
Porphyrin	Monomer (b)	H-aggregate (a)	J-aggregate (c)	Protonated form (d)
$\mathbf{P_1}$	414 ± 1 (4.0)	—	420 ± 1	439 ± 1 (4.4)
$\mathbf{P_2}$	414 ± 1 (3.3)	—	420 ± 1	439 ± 1 (3.7)
$\mathbf{P_3}$	419 ± 3	406 ± 4	442 ± 1	449 ± 3
$\mathbf{P_4}$	419 ± 2	407 ± 3	450 ± 2	443 ± 2
$\mathbf{P_5}$	420 ± 4	405 ± 6	441 ± 4	448 ± 3
$\mathbf{P_6}$	412 ± 4	—	436 ± 3	440 ± 4
TMPyP	424 (2.3)[a]	—	—	447[b]
TPPS	412 (5.3)[a]	405 ± 2	—	434 (6.3)[a]

[a] Literature value.[39] [b] Literature value.[41]

Soret bands of $\mathbf{P_5}$ and $\mathbf{P_6}$ are considerably broadened even at concentrations below 1 μM.

The absorption maximum of band b (Fig. 2) and its predominant presence at low porphyrin concentrations in neutral media are typical for monomeric porphyrins. The Beer–Lambert plots measured for the band b of $\mathbf{P_1}$ and $\mathbf{P_2}$ were linear up to 4 μM yielding extinction coefficients comparable to those of monomeric free-base porphyrins (Table 1).[39] These results show that $\mathbf{P_1}$ and $\mathbf{P_2}$ monomers constituted the dominant solution phase species, at least for the first forty minutes after preparation. The Beer–Lambert plots for $\mathbf{P_3}$–$\mathbf{P_6}$ were non-linear, rather a downward curvature was observed that points to rapid aggregation even at concentrations less than 10^{-7} M. This phenomenon was especially pronounced for $\mathbf{P_5}$ and $\mathbf{P_6}$. Efforts were thus made to assign the nature of resulting aggregates.

Two generalized aggregate structures, H-aggregates and J-aggregates, have been recognized for water soluble porphyrins.[40] The transition dipole moments of monomers interacting in H-aggregates are *perpendicular* to the line connecting their centers, producing a characteristic blue shift of the Soret band. The anionic porphyrin TPPS exclusively exhibits this aggregation mode at high ionic strength (Table 1,a). Blue shifted bands indicative of H-aggregates were also found for $\mathbf{P_3}$–$\mathbf{P_5}$ (Table 1,a). The absorption spectra of $\mathbf{P_1}$ and $\mathbf{P_2}$ also exhibited blue shifted bands, though these are believed to be low intensity vibrational bands rather than H-aggregates. In contrast, the transition dipole moments of monomers interacting in J-aggregates are *parallel* to the line connecting their centers, and are characterized by a red shifted Soret band. This geometry leads to band sharpening relative to H-aggregates, a feature observed in the red shifted Soret band c of $\mathbf{P_1}$–$\mathbf{P_6}$ (Fig. 2). While H-aggregates break up rapidly upon dilution, J-aggregates were found to be very stable, dissociating to monomers very slowly especially in neutral and basic media. As indicated in Table 1, porphyrins $\mathbf{P_1}$–$\mathbf{P_6}$ form J-aggregates while TMPyP does not, an observation consistent with the literature.[41] Similarly, TPPS does not exhibit this mode of aggregation in neutral media.

The formation of J-aggregates occurs much more slowly; in pure water equilibrium is not achieved even after several days. The concentration of J-aggregates and their rates of formation are increased by the addition of NaCl (increased ionic strength), by the addition of phosphate buffer, and by vigorous stirring. This effect is especially pronounced for the phosphonium and sulfonium porphyrins. Contrary to the results of Jin *et al.*,[22] we found a red shifted Soret subband c indicative of J-aggregates for porphyrins containing nitrogen atoms in the *meso*-phenyl substituents ($\mathbf{P_1}$, $\mathbf{P_2}$). However, the aggregate formation was observed only after 30 minutes of intensive stirring. The rate constants of J-aggregate formation, which are dependent on the substituent on the *meso*-phenyl ring, decrease in the following order:

$$\mathbf{P_2} < \mathbf{P_1} \lll \mathbf{P_4} < \mathbf{P_5} \leq \mathbf{P_3} \leq \mathbf{P_6}$$

Theory[42] predicts that the width of the J-aggregate absorption band is narrower than that of the monomer by the factor $N^{1/2}$, where N is the average aggregation number.[43] For example, the absorption spectrum of the solution of $\mathbf{P_4}$ has a J-aggregate band width of ~550 cm^{-1} and a monomer band width of ~1300 cm^{-1} (Fig. 2c, b), therefore any given porphyrin is in direct communication with an average of ~4–5 of its neighbors (N = 5.6). The actual number of monomers within each aggregate can be, however, very high. This is supported by considerable enhancement of resonance light-scattering intensity and by increased baseline offset in the absorption spectra. Aggregates with many monomer units are presumably stabilized by electrostatic forces and by π–π stacking. It is reasonable to assume that the methylene bridge between the phenyl group and the cationic center in $\mathbf{P_1}$–$\mathbf{P_6}$ provides conformational flexibility to accommodate suitable orientation for aggregation.

The longest wavelength peak d (Fig. 2) is observed only at pH less than 5.5 and is associated with the diacid $H_2\mathbf{P_i}^{2+}$ with protonated pyrrole nitrogens [eqn. (1)].

$$\mathbf{P_i} \underset{pK_1}{\overset{H^+}{\rightleftharpoons}} H\mathbf{P_i}^{+} \underset{pK_2}{\overset{H^+}{\rightleftharpoons}} H_2\mathbf{P_i}^{2+} \quad (1)$$

UV–VIS absorption spectrum of $H_2\mathbf{P_i}^{2+}$ consists of only two bands in the visible region due to its high symmetry (D_{4h}). In contrast, the less symmetric (D_{2h}) free-base form $\mathbf{P_i}$ has four absorption bands in the visible spectrum. The monoprotonated form $H\mathbf{P_i}^{+}$ was not distinguished spectrophotometrically, presumably because the pK_1 and pK_2 values for $\mathbf{P_1}$–$\mathbf{P_6}$, like those of the sulfonated analogue TPPS,[39] are so close that the porphyrins exist predominantly in either the free-base or diprotonated forms. The spectral analysis of bands belonging to $\mathbf{P_i}$ (Fig. 2, b) and $H_2\mathbf{P_i}^{2+}$ (Fig. 2, d) under conditions where J-aggregation is minimized allowed the calculation of the apparent dissociation constants ($pK_a = \sqrt{pK_1 \cdot pK_2}$) for $\mathbf{P_1}$ and $\mathbf{P_2}$. The values calculated for $\mathbf{P_1}$ (pK_a 4.8 ± 0.1) and $\mathbf{P_2}$ (pK_a 4.7 ± 0.1) are close to the literature value for TPPS (pK_a 4.9).[39] The electron withdrawing effect of the positively charged groups on the basicity of porphyrins $\mathbf{P_1}$ and $\mathbf{P_2}$ is negligible due to the presence of the methylene bridge between the substituent and the phenyl ring. A comparable system without the insulating methylene bridge, TPP tetrasubstituted in the *para*-phenyl position with $-N^+(CH_3)_3$, is almost two orders of magnitude more acidic (pK_a 3.0).[43] The pyridinium containing TMPyP, where the positive charge is another step closer to the π-system, is even more acidic (pK_a 1.0).[39]

Titration of $H_2\mathbf{P_3}^{2+}$–$H_2\mathbf{P_6}^{2+}$ with NaOH led to the formation of species with an absorption band between 400 and 410 nm similar to the band of the H-aggregate (pH ≥ 2.5) rather than to the recovery of free-base monomer. The observed baseline offset in the spectra of $\mathbf{P_3}$–$\mathbf{P_6}$ and their increased resonance light-scattering indicate the presence of extremely large aggregates in basic solutions (pH > 10).

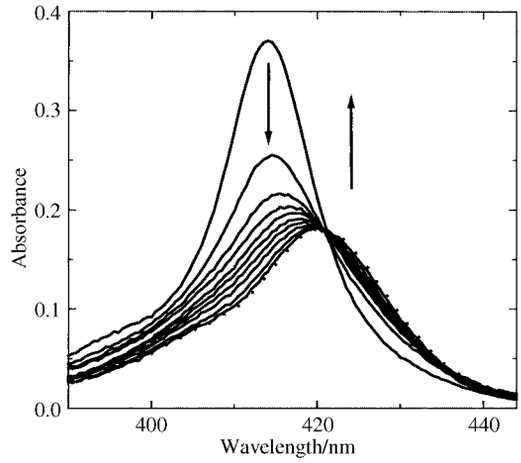

Fig. 3 Spectral titration of 1.5 μM $\mathbf{P_1}$ with DNA. Arrows designate changes in the Soret band, r_0 down to 0.018 (dotted line). 20 mM phosphate buffer, pH 7.0, 100 mM NaCl, corrected for dilution.

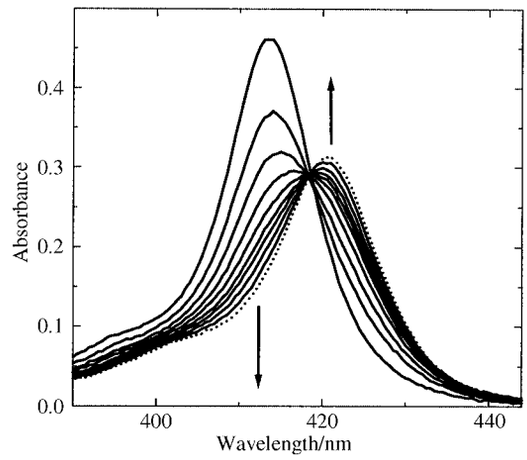

Fig. 4 Spectral titration of 1.4 μM $\mathbf{P_2}$ with DNA. Arrows designate changes in the Soret band, r_0 down to 0.025 (dotted line). 20 mM phosphate buffer, pH 7.0, 100 mM NaCl, corrected for dilution.

The diprotonated porphyrin H_2TPPS^{2+}, which has a net charge of (−2) because of the four anionic sulfonate groups, readily forms J-aggregates at high ionic strength.[44] In contrast, no spectral evidence for the formation of J-aggregates of H_2TMPyP^{2+} (ref. 43) or $H_2\mathbf{P_1}^{2+}$–$H_2\mathbf{P_6}^{2+}$ (<4 μM) was found.

Fluorescence emission spectra of $\mathbf{P_1}$–$\mathbf{P_6}$ have two maxima at ~655 nm and ~720 nm; their position is not affected by aggregation.

C. Interaction with DNA and mononucleotides in water and phosphate buffer

The spectral properties of porphyrins, titrated with aliquots of double-stranded DNA (dsDNA), were measured in the range of 250–800 nm as a function of r_0 (the ratio of total molar concentration of porphyrin to that of dsDNA in base pairs). While the Q-bands of these porphyrins did not shift significantly upon addition of DNA, the Soret band exhibited changes allowing quantitation of porphyrin–DNA binding. Since porphyrins $\mathbf{P_1}$ and $\mathbf{P_2}$ are predominantly monomeric in phosphate buffer (Table 1), it is reasonable to presume that spectral perturbations upon addition of dsDNA are due to association of the porphyrins with the DNA matrix (Fig. 3, 4). This interaction is characterized by a red shift of the Soret maximum to 421 nm ($\varepsilon = 2.0 \times 10^5$ M^{-1} cm^{-1} for $\mathbf{P_1}$ and $\varepsilon = 2.2 \times 10^5$ M^{-1} cm^{-1} for $\mathbf{P_2}$) and by a large (~50%) hypochromicity. The large hypochromicity suggests that porphyrin π electrons are perturbed considerably by association with DNA. Spectral changes show a single isosbestic point, typical of a simple equilibrium between unbound and bound porphyrin (Fig. 3, 4). These forms are also distinguishable by their different diffusion properties, which are manifested in quenching of their triplet states by oxygen. Transient triplet–triplet spectra of $\mathbf{P_1}$ and $\mathbf{P_2}$ have broad absorption maxima typical for porphyrins at 450 nm, which are not affected by DNA binding. In air-saturated solutions, the triplet states are quenched by oxygen monoexponentially with lifetime of 1.5 μs (Fig. 5a). At $r_0 = 0.13$, the unbound and bound porphyrins each have distinct triplet state quenching kinetics with lifetimes of 1.5 μs and 18 μs respectively (Fig. 5b). At higher DNA concentrations ($r_0 = 0.02$, Fig. 5c), three distinct excited triplet states of porphyrin were apparent; one unbound and two bound components. The two bound triplet states were characterized by lifetimes of 7.7 μs and 30 μs, which is probably due to porphyrin in different DNA microenvironments.

Spectral features of TMPyP–DNA complexes have been reported.[3,24] We found a similar bathochromic shift of the Soret band from 424 nm ($\varepsilon_{424} = 2.3 \times 10^5$ M^{-1} cm^{-1}) to 435 nm ($\varepsilon_{435} = 1.6 \times 10^5$ M^{-1} cm^{-1}) concomitant with a large hypochromicity (not shown). The difference between oxygen quenching of the triplet states of TMPyP in the bound and unbound form[26] is similar to above reported for $\mathbf{P_1}$ and $\mathbf{P_2}$.

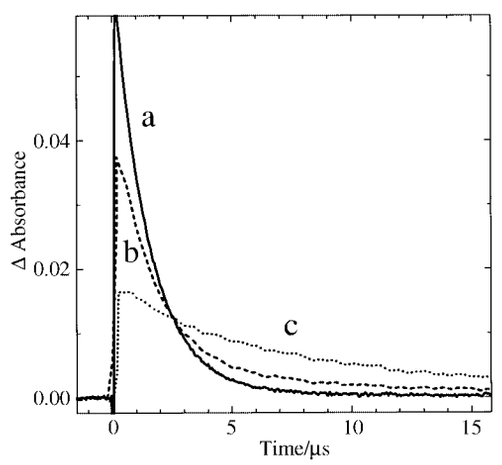

Fig. 5 Quenching of the transient absorption of the $\mathbf{P_1}$ triplet states by oxygen: no DNA (a); DNA, $r_0 = 0.13$ (b, dashed line); DNA, $r_0 = 0.02$ (c, dotted line). Excitation wavelength 412 nm, monitored at 450 nm. 2.8 μM $\mathbf{P_1}$, 20 mM phosphate buffer, pH 7.0, 100 mM NaCl, corrected for dilution.

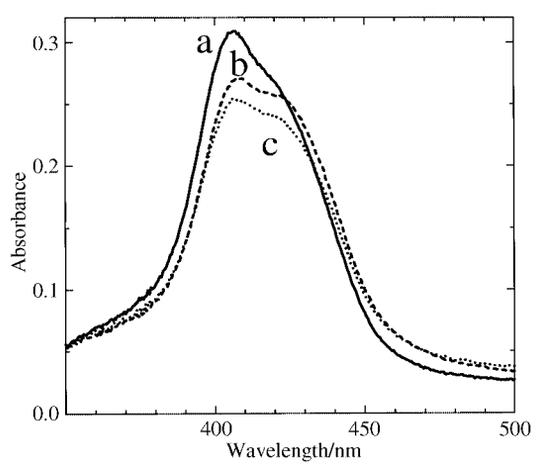

Fig. 6 Soret region of 2.8 μM $\mathbf{P_6}$: no DNA (a); DNA, $r_0 = 0.035$ (b); addition of phosphate buffer (c). 20 mM phosphate buffer, pH 7.0, 100 mM NaCl.

The addition of DNA does not perturb the spectra of $\mathbf{P_3}$–$\mathbf{P_6}$ (Fig. 6), presumably because of extensive self-stacking. The Soret bands are broad with and without DNA, indicating

Table 2 Binding parameters of $\mathbf{P_1}$–$\mathbf{P_6}$ with dsDNA in 20 mM phosphate buffer (pH 7.0, 100 mM NaCl). Apparent binding constants K_a and the number of inaccessible residues n were evaluated using eqn. (3). Binding constants K_a for porphyrin–nucleotide complexes (AMP, GMP) in methanol calculated according to eqn. (2)

	K_a/M^{-1} (n)		
Porphyrin	DNA	AMP	GMP
TPPS	N[a]	N[a]	N[a]
TMPyP	$(1.3 \pm 0.2) \times 10^6$ (2.7) 7.7×10^5 (1.8)[b]	$(6.8 \pm 0.5) \times 10^3$	$(7.3 \pm 0.5) \times 10^3$
$\mathbf{P_1}$	$(1.2 \pm 0.2) \times 10^6$ (8.1)	$(6.7 \pm 0.6) \times 10^3$	$(2.1 \pm 0.3) \times 10^3$
$\mathbf{P_2}$	$(2.1 \pm 0.3) \times 10^6$ (6.2)	$(1.5 \pm 0.3) \times 10^3$	$(7.5 \pm 0.9) \times 10^3$
$\mathbf{P_3}$	N[a]	N[a]	N[a]
$\mathbf{P_4}$	N[a]	Y[c]	Y[c]
$\mathbf{P_5}$	N[a]	N[a]	Y[c]
$\mathbf{P_6}$	N[a]	N[a]	N[a]

[a] Absorption and emission fluorescence spectroscopy gives no evidence of binding. [b] Literature value.[24] [c] Complex porphyrin–nucleotide is observed, however, low absorbance changes ($\Delta A < 0.02$/1 cm cell) do not allow evaluation of K_a according to eqn. (2).

extensive J-aggregation. Further support for this assertion comes from the fact that the quantum yields of the triplet states (Φ_T) of $\mathbf{P_3}$–$\mathbf{P_6}$ are two orders of magnitude lower in buffer than in organic solvents, where $\mathbf{P_3}$–$\mathbf{P_6}$ are predominantly monomeric. It is well known[45] that the quantum yields of the triplet states decrease dramatically when aggregation occurs. In summary, the high stability of J-aggregates of $\mathbf{P_3}$–$\mathbf{P_6}$ in aqueous solutions either renders the porphyrins unavailable for binding biological substrates or prevents the binding event from causing a change measurable spectroscopically. TPPS, the only anionic porphyrin studied, does not exhibit any sign of interaction with DNA (nor nucleotides).

Absorption spectra of TMPyP, $\mathbf{P_1}$ and $\mathbf{P_2}$ were analyzed according to the McGhee–von Hippel model for binding of non-interacting ligands to a lattice of binding residues [eqn. (3)]. The free porphyrin concentration m for different values of r_0 can be calculated reliably and was verified by several independent experiments. The binding constants K_a and the exclusion parameters n were obtained from the linear limiting part of the binding isotherms at low r according to Pasternack *et al.*[24] The values of K_a and n are summarized in Table 2. TMPyP is known to intercalate at GC sites with an apparent binding constant[24] K_a of 7.7×10^5 M^{-1}. Outside (non-intercalated) binding, predominantly at AT sites, occurs at high porphyrin/DNA ratios (r_0) and at high ionic strength.[3] Our experiment, which uses low TMPyP loading to promote intercalation over outside binding, yields a comparable binding constant ($K_a = 1.3 \times 10^6$ M^{-1}). Surprisingly, $\mathbf{P_1}$ and $\mathbf{P_2}$ have apparent binding constants of the same order of magnitude (Table 2) in spite of the structural differences between these compounds and TMPyP.

Absorption and fluorescence emission spectra of $\mathbf{P_3}$–$\mathbf{P_6}$ indicate the porphyrins are highly self-aggregated and do not form nucleotide complexes in buffer in the presence of a large excess of AMP, GMP, CMP or TMP (up to 1 mM as limited by solubility). Weak complexes cannot be, however, excluded since all porphyrins bear high positive charge. Under the same conditions, TMPyP forms stacking-type complexes with nucleotides with binding constants up to 10^3 M^{-1}.[36,46] The stronger complexes are formed with double ring purine bases, presumably due to more extensive π–π overlap than with the single-ring pyrimidine bases.

D. Binding modes: induced CD spectra and molecular biology study

Circular dichroism (CD) spectroscopy (Fig. 7) was employed to ascertain the effect of the stereogenic DNA environment on cationic porphyrins $\mathbf{P_1}$–$\mathbf{P_6}$. The binding modes between porphyrins and DNA are governed by porphyrin shape and charge and by DNA sequence, as documented by extensive research

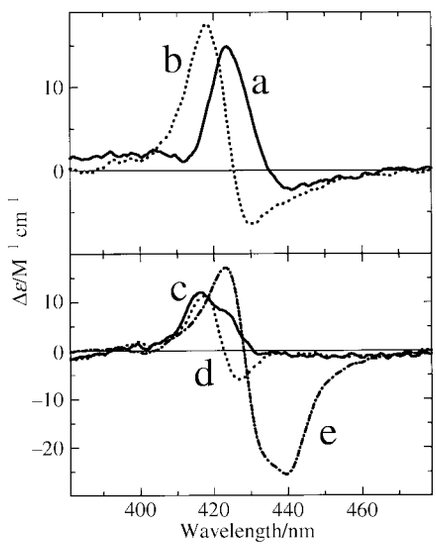

Fig. 7 Induced circular dichroism spectra of $\mathbf{P_1}$ (2.7 μM), $\mathbf{P_2}$ (1.6 μM) and $\mathbf{P_4}$ (4.1 μM) with DNA. $\mathbf{P_1}$: $r_0 = 0.346$ (a), $r_0 = 0.003$ (b). $\mathbf{P_2}$: $r_0 = 0.078$ (c), $r_0 = 0.002$ (d). $\mathbf{P_4}$: $r_0 = 0.005$ (e). 20 mM phosphate buffer, pH 7.0, 100 mM NaCl.

on free-base and metallated forms of TMPyP.[3,24] Intercalative and external groove binding modes have been associated with negative and positive induced Soret CD bands, respectively. $\mathbf{P_1}$–$\mathbf{P_6}$ are achiral and hence no CD spectra were displayed in buffer in the absence of DNA. In the presence of DNA, porphyrins $\mathbf{P_1}$ (Fig. 7a,b) and $\mathbf{P_2}$ (Fig. 7c,d) have similar circular dichroic features and display a sensitivity to porphyrin loading r_0. At high values of $r_0 > 0.3$, a single positive peak centered at 424 nm is observed. With further addition of DNA ($0.015 > r_0 > 0.3$) a new positive signal appears at 418 nm. The intensity of this peak increases with decreasing r_0 and at $r_0 < 0.03$ is the only peak present ($\Delta\varepsilon = 23.5$ M^{-1} cm^{-1} for $\mathbf{P_1}$ and $\Delta\varepsilon = 12.2$ M^{-1} cm^{-1} for $\mathbf{P_2}$). Low intensity negative peaks at 430 nm ($\mathbf{P_1}$) and 427 nm ($\mathbf{P_2}$) are observed under extreme porphyrin/DNA dilution ($r_0 = 0.003$ or 0.002). The appearance of two positive bands at low r_0 suggests a high binding affinity of $\mathbf{P_1}$ and $\mathbf{P_2}$ for DNA and a number of possible outside binding configurations at both GC and AT sequences. Evidently, the binding preference depends upon porphyrin loading. This was observed recently for MnTMPyP where the shorter and the longer wavelength peaks are assigned to the minor and to the major groove binding modes.[47] $\mathbf{P_1}$ and $\mathbf{P_2}$ do not display a conservative CD spectrum that excludes the presence of long range assemblies of stacked porphyrin units arranged into helical domains on DNA. In accordance with it, having employed the resonance light scattering[35] we did not find any enhancement of scattered

light intensity. However, induced CD spectra at $r_0 = 0.002$ look like exciton splitting with a few porphyrin units in close contact. Strong porphyrin based signal of $\mathbf{P_4}$ (Fig. 7e) is commonly attributed to highly ordered outside stacking binding mode originally proposed by Fiel.[3]

Under conditions of low porphyrin loading $r_0 < 0.1$ and low ionic strength, intercalation of porphyrins into calf thymus DNA generally induces a negative CD band in the Soret region.[24,48] Thus, the CD spectra provided no evidence for $\mathbf{P_1}$–$\mathbf{P_6}$ intercalation. A biochemical study, involving a topoisomerase I assay, corroborates this conclusion.[49] This study measures the unwinding of the dsDNA helix induced by small molecules, a classic signature of DNA intercalation. Unwinding of supercoiled pBR322 DNA was not induced by porphyrins $\mathbf{P_1}$, $\mathbf{P_5}$ or $\mathbf{P_6}$.

CD and biochemical measurements of the porphyrin–DNA binding fit the McGhee–von Hippel model well [eqn. (3)]. Apparent binding constants of $\mathbf{P_1}$ and $\mathbf{P_2}$ with DNA are comparable to the intercalation affinity of TMPyP (Table 2). However, these high K_a values are not necessarily indicative of intercalation and can only confirm[3e] that porphyrins $\mathbf{P_1}$ and $\mathbf{P_2}$ exhibit a large binding affinity for DNA. The number of DNA base pairs (n) covered by $\mathbf{P_1}$ ($n = 8.1$) and $\mathbf{P_2}$ ($n = 6.2$) is much higher than that of TMPyP ($n = 2.7$) and corroborates the supposition that they do not intercalate but rather bind to the outside surface of DNA. We assume $\mathbf{P_1}$ and $\mathbf{P_2}$ are too large to intercalate extensively since n increases with increasing steric bulk in the *meso*-positions (TMPyP < $\mathbf{P_2}$ < $\mathbf{P_1}$). Modeling indicates porphyrins $\mathbf{P_1}$ and $\mathbf{P_2}$ have a diameter exceeding 1.5 nm. If we assume that the porphyrin binds to the phosphate backbone along the major groove such that the plane of the macrocycle is parallel to the helix axis, as proposed by Fiel *et al.*,[3] and that adjacent base pairs are separated by about 0.34 nm (B–DNA), the porphyrin should cover an area about five base pairs in length. The values of $n = 8.1$ and 6.2 for $\mathbf{P_1}$ and $\mathbf{P_2}$, respectively, are in accord with this predicted value.

The interactions between highly hydrophobic porphyrins $\mathbf{P_3}$–$\mathbf{P_6}$ and DNA cannot be easily studied using UV–VIS spectroscopy because of the extensive degree of porphyrin aggregation. CD spectroscopy does show that $\mathbf{P_4}$ is bound externally as stacked units on the exterior surface of DNA. In conclusion, porphyrins $\mathbf{P_1}$–$\mathbf{P_6}$ do not intercalate but rather bind to the surface of DNA helices *via* two binding modes.

E. Interaction with mononucleotides in methanol; sensitized decomposition of GMP

In general, the porphyrins studied have a much lower tendency to aggregate in methanol than in buffer. The extensive hypochromicity of the Soret band observed for TMPyP, $\mathbf{P_1}$ and $\mathbf{P_2}$ indicates that these porphyrins bind GMP and AMP (Table 2). The complexation is also accompanied by a red shift of about 1–2 nm for $\mathbf{P_1}$ and $\mathbf{P_2}$ and about 3 nm for TMPyP. We assume that the electronic structure of the monomeric porphyrins is not greatly affected by interaction with nucleotides because the methylene bridge separates the positively charged moiety (the presumed nucleotide binding site) and the porphyrin chromophore. Spectral features observed are typical for a binary equilibrium with clear isosbestic points. Spectral analysis [eqn. (2)] indicates that these porphyrins have a high affinity for GMP and AMP, with binding constants *ca.* $2–8 \times 10^3$ M^{-1} (Table 2). No significant spectral changes were observed for $\mathbf{P_3}$–$\mathbf{P_6}$ in the presence of nucleotides, either because they do not bind or because the binding does not perturb the porphyrin chromophore. The same is true of TPPS, though in this case it is reasonable to assume there is no binding interaction between the two anionic species.

GMP was chosen as a model for the compounds of biological interest that would be potential targets of porphyrin photosensitization because it binds the porphyrins more strongly than CMP and TMP[36] and because guanine is believed to be the site of singlet oxygen attack in the photodynamic destruction of DNA.[27–29] Fast electron transfer between the excited singlet state of bound TMPyP and guanine residues has been also reported.[36] The relative contribution of these pathways[50–52] can be controlled by reaction conditions, especially by the presence of dissolved oxygen. The effect of oxygen is evident from the measurement of the porphyrin triplet states. Triplets of TPPS, TMPyP and $\mathbf{P_1}$–$\mathbf{P_6}$, have long lifetimes in methanol (>0.5 ms in oxygen-free solution) and they are effectively quenched by oxygen with bimolecular rate constant $k_{O2} \sim 10^9$ M^{-1} s^{-1} to form singlet oxygen $^1O_2$. The formation of $^1O_2$ was directly measured of its specific luminescence at 1270 nm. In air-saturated solution, quenching of the triplet states by GMP was not observed. Thus, the triplet lifetime of ~300 ns was only governed by quenching with oxygen, meaning that the dominant process responsible for decomposition of GMP in air-saturated solution is the oxidative attack by singlet oxygen rather than energy or electron transfer.

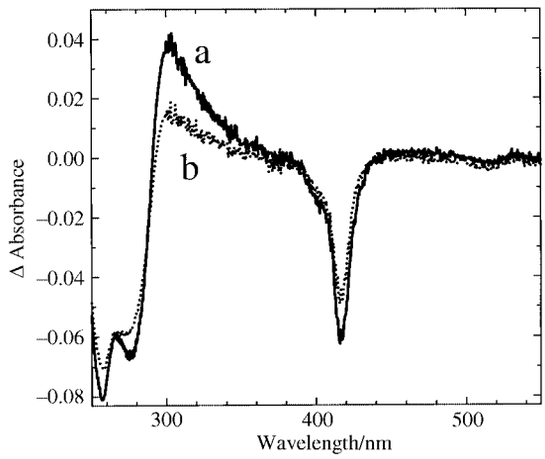

Fig. 8 Difference absorption spectra of 2.7 μM $\mathbf{P_6}$ in the presence of 50 μM GMP after 120 minutes of irradiation by an Ar^+ laser ($\lambda_{exc} = 514.5$ nm, 95 mW) in air-saturated (a) and in oxygen-free methanol (b).

Continuous irradiation of TMPyP, TPPS and $\mathbf{P_1}$–$\mathbf{P_6}$ by an Ar^+-laser light in air-saturated methanol leads to GMP decomposition as evidenced by forming of a broad absorption band above 300 nm (Fig. 8a). Since in air-saturated solutions the decomposition of GMP occurs predominantly *via* singlet oxygen mechanism, we can compare the sensitizing abilities of respective porphyrins. Unfortunately, calculation of the decomposition rate constants is not possible due to the overlap of absorption spectra of GMP and its various degradation products. It was clear, however, that cationic porphyrins TMPyP and $\mathbf{P_1}$–$\mathbf{P_6}$ (Fig. 9a–g) sensitize the decomposition of GMP faster than the anionic TPPS does (Fig. 9h). TMPyP and $\mathbf{P_2}$ show the highest sensitization (Fig. 9a, b), presumably because these compounds have relatively high binding affinity for GMP (Table 2). In conclusion, the association of cationic porphyrins and GMP facilitates nucleotide decomposition since the highly reactive singlet oxygen generated at the porphyrin chromophore is in close proximity to GMP.

We found that porphyrin-sensitized GMP decomposition took place also under oxygen-free conditions (Fig. 8b), indicating energy and/or electron transfer between the excited states of the porphyrins and GMP. Jasua *et al.*[36] reported thermodynamic data consistent with electron transfer between guanine base and TMPyP, and it is reasonable to assume a similar quenching process occurs with $\mathbf{P_1}$ and $\mathbf{P_2}$. The kinetics of the deactivation of the triplet states of $\mathbf{P_1}$–$\mathbf{P_6}$ were monoexponential with lifetimes of 600–800 μs in oxygen-free conditions. In the presence of 0.8 mM GMP, the data for the triplet states fit biexponential rather than monoexponential decay kinetics. The

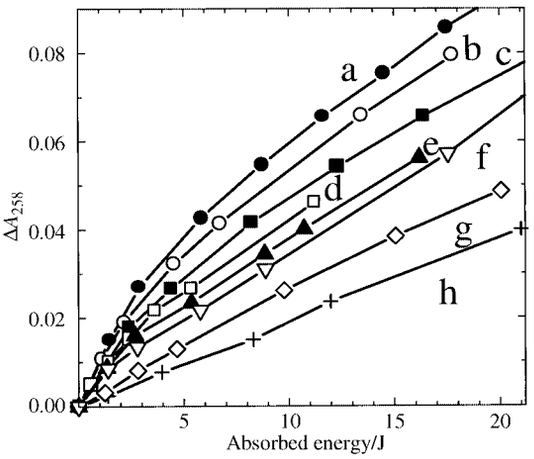

Fig. 9 Photosensitized decomposition of 50 μM GMP in methanol as monitored from decrease of the GMP absorption peak at 258 nm. Expressed as a function of absorbed energy by TMPyP (a), $\mathbf{P_2}$ (b), $\mathbf{P_3}$ (c), $\mathbf{P_4}$ (d), $\mathbf{P_5}$ (e), $\mathbf{P_6}$ (f), $\mathbf{P_1}$ (g) and TPPS (h). Irradiated by an Ar^+ laser (λ_{exc} = 514.5 nm, 95 mW, *ca.* 2.7 μM porphyrins with matching absorbance at λ_{exc}, ~0.05/10 mm cell).

rate constant of the slower process matched that of the triplet state decay in the absence of GMP. The rate constant of the faster process, 200–300 μs, was dependent on the porphyrin substituent. These triplet states were assigned to the triplet states of the porphyrin–GMP complex that are believed to be responsible for GMP decomposition. On the other hand, no influence of GMP on the triplet states of anionic TPPS was found due to Coulombic repulsion which prevents formation of a complex between TPPS and GMP. Therefore, any possible interaction between the triplets of TPPS and the nucleotide can occur only by less efficient collisional mechanism.

Conclusion

Cationic *meso*-tetraphenyl porphyrins *para*-substituted with $-CH_2(pyridinio)^+$ ($\mathbf{P_1}$) and $-CH_2N^+(CH_3)_3$ ($\mathbf{P_2}$) groups form complexes with dsDNA (K_a ~10^6 M^{-1}). In contrast to TMPyP, a known GC intercalator, $\mathbf{P_1}$ and $\mathbf{P_2}$ form complexes with DNA *via* the external binding mode. This is most likely due to the larger size of the *meso*-substituents. Porphyrins with positively charged phosphorus or sulfur atoms ($\mathbf{P_3}$–$\mathbf{P_6}$) in the *meso*-substituent form stable homoaggregates in aqueous solution, especially at higher ionic strengths. Binding of these aggregates with the exterior of dsDNA cannot be followed by spectrophotometric methods since there is no observable change upon binding. We know from CD experiments that $\mathbf{P_4}$ is bound externally in the form of stacked units. $\mathbf{P_1}$–$\mathbf{P_6}$ are generally less efficient sensitizers for decomposition of negatively charged molecules of biological interest (nucleotides) than TMPyP, perhaps because they extensively aggregate. In methanol the cationic porphyrins do not readily aggregate with each other but form sandwich-type complexes with nucleotides that are electrostatically stabilized. When a nucleotide-complexed porphyrin is photoexcited, singlet oxygen is produced in close proximity to the nucleotide, generally leading to its decomposition.

Experimental

Materials

The tetrasodium salt of *meso*-tetrakis(4-sulfonatophenyl)-porphyrin (TPPS) and tetratosylate of *meso*-tetrakis(4-*N*-methylpyridyl)porphyrin (TMPyP) were purchased from Porphyrin Products, Utah, USA. The stock solutions of porphyrins were prepared in dimethyl sulfoxide (DMSO, spectrophotometric grade, Aldrich) and diluted with water, phosphate buffer, or methanol prior to use. The concentration of porphyrins was below 5 μM and DMSO content did not exceed 5% v/v. In the acid–base experiments the pH values were adjusted by using 0.1 M NaOH or 0.1 M HCl as appropriate. Adenosine 5′-monophosphate (AMP), guanosine 5′-monophosphate (GMP), cytidine 5′-monophosphate (CMP) and thymidine 5′-monophosphate (TMP) (all disodium salts from yeasts, Sigma) were used without purification. The concentration of calf thymus double-stranded DNA (Sigma), calculated in base pairs, was determined spectrophotometrically using molar absorptivity $\varepsilon_{260} = 1.31 \times 10^4$ $M^{-1}cm^{-1}$.[33]

Spectral measurements

The laser kinetic spectrometer (Applied Photophysics, UK) as well as the details of measurement have been described elsewhere.[34] A Lambda Physik FL 3002 dye laser (λ_{exc} = 413 nm, pulse length 28 ns, output 1–5 mJ per pulse) was used for production of the triplet states. The porphyrin triplets were probed at 444 nm using a 250 W Xe lamp equipped with a pulse unit and a R928 photomultiplier (Hamamatsu). Time-resolved near-infrared emission at 1270 nm belonging to singlet oxygen $O_2(^1\Delta_g)$ was monitored with a Ge diode (Judson J16-8SP, USA) in conjunction with an interference filter. Where appropriate, oxygen was removed from solution *via* argon purging. Continuous irradiation experiments of porphyrin–GMP solutions were carried out with the green line of an Ar^+ laser (λ = 514.5 nm, output power 95 mW, Coherent Innova 200). All experiments were performed in 10 mm quartz cells immediately after sample preparation to minimize the effect of self-aggregation and adsorption of the porphyrins on to the cell walls. Porphyrins $\mathbf{P_1}$–$\mathbf{P_6}$ had less of a tendency to "plate out" onto the quartz cell than TMPyP. This effect does not appear to influence the experimental results.

The induced CD spectra of porphyrins were measured on a Jobin Yvon-Spex CD 6 at selected porphyrin : DNA ratios (r_0). All spectra were obtained by averaging three accumulations recorded with steps of 0.5 nm (1 s integration time). Steady state fluorescence emission spectra were recorded on a Perkin-Elmer LS 50B luminescence spectrophotometer. The samples were excited at the visible $Q_y(1,0)$ absorption band (usually 515 nm) because it is less influenced by binding than the Soret band. Resonance light-scattering experiments[35] were conducted using simultaneous scans of the excitation and emission monochromators through the range of 300 to 600 nm.

UV/VIS absorption spectra were measured using a Lambda 19 absorption spectrometer (Perkin-Elmer). Absorbance titrations were conducted by adding concentrated stock solution of DNA or nucleotides directly to a porphyrin solution in a cuvette. Experiments with different porphyrin : DNA concentration ratios (r_0) were performed in solutions containing 20 mM phosphate buffer (pH 7.0) and 100 mM sodium chloride at room temperature (25 °C). The apparent binding constants K_a for porphyrin–nucleotide complexes were calculated from the absorbance changes at the Soret maximum (ΔA) assuming a 1 : 1 stoichiometry and that the nucleotide concentration N is always significantly larger than the porphyrin concentration [eqn. (2)].[36]

$$\frac{1}{\Delta A} = \frac{1}{K_a N(\Delta A)_\infty} + \frac{1}{(\Delta A)_\infty} \qquad (2)$$

$(\Delta A)_\infty$ represents the extrapolated absorbance change at $N \rightarrow \infty$. The binding of porphyrins to DNA was evaluated using a McGhee–von Hippel model[24,37] which incorporates neighbor exclusion effects for the binding of a molecule to homogeneous one-dimensional lattices [eqn. (3)], where r is the ratio of molar

$$\frac{r}{m} = K_a(1 - nr)\left[\frac{1 - nr}{1 - (n-1)r}\right]^{n-1} \qquad (3)$$

concentration of bound porphyrin to total molar concentration of DNA in base pairs, m is the free porphyrin molar concentration. The exclusion parameter n, expressed in base pairs, is the number of potential binding sites removed by the binding event. Values of r and m were calculated from absorption spectra assuming that the porphyrin is completely bound at 20–50-fold excess of DNA.

Syntheses

Solvents and other reagents were purchased from Aldrich Chemical Co. Tetrahydrofuran (THF) and toluene were distilled in the presence of sodium metal. NMR spectra were recorded on a Varian Gemini 300 MHz spectrometer, using solvent as a reference. NMR shifts (δ) are reported in ppm; coupling constants are reported in Hertz. IR spectra were collected on a Nicolet 520 FTIR using KBr technique. Elemental analyses were performed by Analytical Services ICT at Praha. Mass spectra were measured on a ZAB EQ instrument (VG Analytical) in FAB mode (Xe ionization).

5,10,15,20-Tetrakis(α-bromo-*p*-tolyl)porphyrin (P_0). The porphyrin was prepared according to a previously published procedure.[32]

5,10,15,20-Tetrakis(α-pyridinio-*p*-tolyl)porphyrin tetrabromide salt (P_1). 33 mg of P_0 (0.033 mmol) was dissolved in 5 ml of pyridine in a sealed tube and was heated to 100 °C for 10 hours with vigorous stirring. After cooling to room temperature the seal was broken and suspension filtered off. The precipitate was washed with THF–ethanol (2 : 1) and dried. Yield: 43 mg (quantitative). ^{1}H NMR(DMSO-d_6): 9.61 (m, 8H, pyridine), 8.79 (br s, 8H, β-pyrrole), 8.38 (m, 4H, pyridine), 8.29 (m, 8H, phenyl), 8.01 (m, 8H, phenyl), 7.15 (m, 8H, pyridine), 5.77 (br s, 8H, phenyl-CH_2), −2.98 (br s, 2H, NH). ^{13}C NMR(DMSO-d_6): 147.81, 146.71, 144.99, 142.79, 135.97, 133.33, 131.71, 129.16, 128.62, 128.23, 126.08, 119.70, 64.99. MS: 984 (MH^+ + 1) ($C_{68}H_{54}N_8$; 982.5). UV–VIS (CH_3OH): 415 (Soret, $\varepsilon = 2.8 \times 10^5$ $M^{-1}cm^{-1}$), 513, 546, 590, 647 nm. For $C_{68}H_{54}N_8Br_4$ (1302.830) was calculated: H: 4.18%; C: 62.89%; N: 8.60%; found: H: 4.21%; C: 63.47%; N: 8.47%.

5,10,15,20-Tetrakis(α-trimethylammonio-*p*-tolyl)porphyrin tetrabromide salt (P_2). 33 mg of P_0 (0.033 mmol) was suspended in 5 ml of trimethylamine (31–35% solution in ethanol, Fluka) in a sealed tube. The resulting cloudy solution was heated to 80 °C for 14 hours with vigorous stirring. After cooling to room temperature, the seal was broken and the suspension filtered. The precipitate was washed with THF–ethanol (2 : 1) and dried. Yield: 40.4 mg (quantitative). ^{1}H NMR (DMSO-d_6): 8.94 (s, 8H, β-pyrrole), 8.36 (m, 8H, phenyl), 8.01 (m, 8H, phenyl), 4.96 (s, 8H, CH_2), 3.31 (s, 36H, CH_3), −2.92 (br s, 2H, NH). ^{13}C NMR (DMSO-d_6): 142.88, 134.63, 131.35, 129.12, 128.78, 128.23, 128.02, 127.85, 119.32, 67.61, 52.02. MS: 904 (MH^+) ($C_{60}H_{70}N_8$; 902.6). UV–VIS (CH_3OH): 415 (Soret, $\varepsilon = 2.5 \times 10^5$ $M^{-1}cm^{-1}$), 513, 546, 590, 647 nm. For $C_{60}H_{70}N_8Br_4$ (1222.870) was calculated: H: 5.77%; C: 58.93%; N: 9.16%; found: H: 5.81%; C: 58.67%; N: 9.17%.

5,10,15,20-Tetrakis(α-tri-*n*-butylphosphonio-*p*-tolyl)porphyrin tetrabromide salt (P_3). To a solution of 33 mg P_0 (0.033 mmol in 20 ml of absolute THF) 0.25 ml of tri-*n*-butylphosphine (1.0 mmol) was added. The solution was refluxed under argon for 14 hours. Toluene (10 ml) was added through a septum and a dark green-violet precipitate was collected by filtration, washed with warm THF and dried under vacuum. Yield: 53.5 mg (89%). ^{1}H NMR($CDCl_3$+CD_3OD): 8.85 (s, 8H, β-pyrrole), 8.24 (m, 8H, phenyl), 7.85 (m, 8H, phenyl), 4.61 (d, 8H, J = 14.47 Hz, phenyl-CH_2), 2.68 (m, 24H, butyl P-CH_2), 1.60 (m, 48H, -$(CH_2)_2$-), 1.06 (t, 36H, J = 7 Hz, butylCH_3), −2.79 (br s, 2H, NH). ^{13}C NMR (DMSO-d_6): 145.46, 142.01, 138.70, 135.34 (d, J = 38 Hz), 130.21, 128.19 (d, J = 51 Hz), 127.93 (d, J = 50 Hz), 127.26, 118.93, 26.51 (d, J = 181 Hz), 23.66 (d, J = 61 Hz), 23.28 (d, J = 18 Hz), 18.41 (d, J = 186 Hz), 12.95. ^{31}P NMR (H decoupled, $CDCl_3$+CD_3OD): 36.21. MS: 1476 (MH^+) ($C_{96}H_{142}N_4P_4$; 1475.0). UV–VIS (CH_3OH): 415 (Soret $\varepsilon = 3.2 \times 10^5$ $M^{-1}cm^{-1}$), 513, 548, 590, 647 nm. For $C_{96}H_{142}N_4Br_4P_4$ (1795.692) was calculated: H: 7.99%; C: 64.33%; N: 3.13%; found: H: 8.11%; C: 65.47%; N: 3.07%.

5,10,15,20-Tetrakis(α-triphenylphosphonio-*p*-tolyl)porphyrin tetrabromide salt (P_4). A Schlenk-type microvial with a septum-sealed inlet was charged with 0.26 g of triphenylphosphine (1.0 mmol) and 33 mg P_0 (0.033 mmol), repeatedly evacuated and flushed with argon, and then heated to 110 °C. The resulting melt was maintained at 110 °C and stirred for 12 h. Absolute toluene (5.0 ml) was added through the septum and the resulting suspension was cooled to 70 °C. A dark brown-violet precipitate was collected by filtration, washed with warm toluene and dried under vacuum. Yield: 67.0 mg (99%). ^{1}H NMR ($CDCl_3$+CD_3OD): 8.79 (s, 8H, β-pyrrole) 8.05 (m, 8H, phenyl-CH_2), 7.97 (m, 36H, P-phenyl), 7.88 (m, 24H, P-phenyl), 7.46 (m, 8H, phenylCH_2), 5.33 (d, 8H, J = 15 Hz, CH_2-P). ^{13}C NMR ($CDCl_3$+CD_3OD): 143.51, 136.65 (d, J = 5 Hz), 136.23, 135.62 (d, J = 35 Hz), 133.77, 133.06 (d, J = 40 Hz), 131.60 (d, J = 50 Hz), 130.85 (d, J = 20 Hz), 129.97 (d, J = 50 Hz), 129.29 (d, J = 30 Hz), 120.71, 119.72, 119.03, 30.60 (d, J = 191 Hz). ^{31}P NMR (H decoupled; $CDCl_3$+CD_3OD): 19.94. MS: 1715 (M^+) ($C_{120}H_{94}N_4P_4$; 1714.6). UV–VIS (CH_3OH): 415 (Soret, $\varepsilon = 3.0 \times 10^5$ $M^{-1}cm^{-1}$), 513, 548, 590, 647 nm. For $C_{120}H_{94}N_4Br_4P_4$ (2035.57) was calculated: H: 4.67%; C: 70.92%; N: 2.76%; found: H: 4.53%; C: 70.2%; N: 2.68%.

5,10,15,20-Tetrakis(α-dimethylsulfonio-*p*-tolyl)porphyrin tetrabromide salt (P_5). 33 mg P_0 (0.033 mmol) was dissolved in 5 ml of dimethyl sulfide in a sealed tube. Resulting solution was heated to 50 °C for 14 hours with vigorous stirring. After cooling to room temperature, the seal was broken and suspension filtered. The precipitate was washed with THF–ethanol (1 : 2) and dried. Yield: 30.7 mg (76%). ^{1}H NMR(DMSO-d_6+CD_3-OD): 8.81 (br s, 8H, β-pyrrole), 8.07 (m, 8H, phenyl), 7.51 (m, 8H, phenyl), 4.48 (d, 8H, phenyl-CH_2), 2.70 (s, 24H, CH_3), −2.83 (br s, 2H, NH). MS: 915 (MH^+) ($C_{56}H_{58}N_4S_4$; 914.4). UV–VIS (CH_3OH): 416 (Soret, $\varepsilon = 2.9 \times 10^5$ $M^{-1}cm^{-1}$), 517, 550, 593, 651 nm. For $C_{56}H_{58}N_4S_4Br_4$ (1234.970) was calculated: H: 4.73%; C: 54.46%; N: 4.54%; found: H: 4.81%; C: 54.67%; N: 4.47%.

5,10,15,20-Tetrakis(α-isothiouronium-2-yl-*p*-tolyl)porphyrin tetrabromide salt (P_6). To a solution of 33 mg P_0 (0.033 mmol in 20 ml of absolute THF) 76 mg of thiourea (1.0 mmol) was added. The solution was refluxed under argon for 14 hours. The dark green precipitate was collected by filtration, washed with warm THF and dried under vacuum. Yield: 42.5 mg (quantitative). ^{1}H NMR (DMSO-d_6): 9.50 (br s, 8H, =NH_2), 9.30 (br s, 8H, -NH_2), 8.84 (s, 8H, β-pyrrole), 8.27 (m, 8H, phenyl), 7,90 (m, 8H, phenyl), 4.94 (s, 8H, CH_2), −2,67 (s, 2H, NH). ^{13}C NMR (DMSO-d_6): 169.27, 140.77, 135.05, 134.63, 131.32, 128.85, 128.15, 127.66, 125.27, 119.54, 34.23. MS: 967 (MH^+), ($C_{52}H_{46}N_{12}S_4$; 966.3). UV–VIS (CH_3OH): 416 (Soret, $\varepsilon = 2.9 \times 10^5$ $M^{-1}cm^{-1}$), 515, 551, 592, 647 nm. IR: ν (NH_2) 3405; ν (NH_2) 3310, 3290; ν (NH) 3178; ν (CH_3) 2953; ν (CH_2) 2855; ν (NH_2^+) 2725, 2608; ν (C=N^+) 1611; ν (pyrrole C=C) 1553; ν (pyrrole C=N) 1474; ν (pyrrole C–N) 1353; ν (C–S) 644 cm^{-1}. For $C_{52}H_{50}N_{12}Br_4S_4$ (1285.990) was calculated: H: 3.92%; C: 48.52%; N: 13.07%; found: H: 4.01%; C: 48.71%; N: 13.19%.

Acknowledgements

This research was supported by the Grant Agency of the Czech Republic (grant No. 203/99/1163), by a fellowship from the

Falk Chair in Laser Phototherapy and by the Faculty of Natural Sciences at Bar Ilan University. Financial support to VK from the Howard Hughes Medical Institute (grant No. 75195-541101), the Grant Agency of the Czech Republic (grant No. 301/98/k042) and the Ministry of Education of the Czech Republic (grant VS 97135) is gratefully acknowledged. We thank Dr H. Votavová for measuring CD spectra and Dr D. M. Wagnerová for her helpful discussions.

References

1 (*a*) E. B. Fleischer, *Inorg. Chem.*, 1962, **1**, 493; (*b*) C. I. Wynter, P. Hambright and C. H. Cheek, *Nature* (*London*), 1967, **216**, 1105; (*c*) P. Hambright and E. B. Fleischer, *Inorg. Chem.*, 1970, **9**, 1757.

2 M. Krishnamurthy, *Indian J. Chem.*, *Sect. B*, 1977, **15**, 964.

3 (*a*) R. J. Fiel, J. C. Howard, E. H. Mark and N. Datta-Gupta, *Nucleic Acids Res.*, 1979, **6**, 3039; (*b*) D. A. Musser, N. Datta-Gupta and R. J. Fiel, *Biochem. Biophys. Res. Commun.*, 1980, **97**, 918; (*c*) M. J. Carvlin, N. Datta-Gupta and R. J. Fiel, *Biochem. Biophys. Res. Commun.*, 1982, **108**, 66; (*d*) R. J. Fiel, T. A. Beerman, E. H. Mark and N. Datta-Gupta, *Biochem. Biophys. Res. Commun.*, 1982, **108**, 1067.

4 (*a*) *Photosensitizing Compounds: Their Chemistry*, *Biology and Clinical Use*, eds. G. Bock and S. Harnett, Wiley, Chichester, UK, 1989; (*b*) *Photodynamic Therapy of Neoplastic Disease*, ed. D. Kessel, vol. 2, CRC Press, Boca Raton, 1990; (*c*) T. J. Dougherty, *Photochem. Photobiol.*, 1993, **58**, 895; (*d*) R. Bonnett, *Chem. Soc. Rev.*, 1995, **24**, 19; (*e*) E. D. Sternberg, D. Dolphin and C. Brückner, *Tetrahedron*, 1998, **54**, 4151.

5 J. C. Dabrowiak, B. Ward and J. Goodisman, *Biochemistry*, 1989, **28**, 3313.

6 R. T. Wheelhouse, D. Sun, H. Han, F. X. Han and L. H. Hurley, *J. Am. Chem. Soc.*, 1998, **120**, 3261.

7 T. Uno, K. Hamasaki, M. Tanigawa and S. Shimbayashi, *Inorg. Chem.*, 1997, **36**, 1676.

8 R. Lauceri, T. Campagna, A. Contino and R. Purrello, *Angew. Chem.*, *Int. Ed. Engl.*, 1996, **35**, 215.

9 N. V. Anantha, M. Azam and R. D. Sheardy, *Biochemistry*, 1998, **37**, 2709.

10 H. Arthanari, S. Basu, T. L. Kawano and P. H. Bolton, *Nucleic Acids Res.*, 1998, **26**, 3724.

11 (*a*) M. Asanaka, T. Kurimura, H. Toya, J. Ogaki and Y. Kato, *AIDS*, (*London*), 1989, **3**, 403; (*b*) D. W. Dixon, L. G. Marzilli and R. Schinazi, *Ann. N.Y. Acad. Sci.*, 1990, **616**, 511; (*c*) J. L. Sessler, M. J. Cyr, B. G. Maiya, M. Judy, J. T. Newman, H. L. Skiles, R. Boriak, J. L. Matthews and T. C. Chanh, *Proc. SPIE-Int. Opt. Eng.*, 1990, **1203**, 233; (*d*) R. D. Levere, Y. F. Gong, A. Kappas, D. J. Bucher, G. P. Womser and N. G. Abraham, *Proc. Acad. Natl. Sci. U.S.A.*, 1991, **88**, 1756; (*e*) A. K. Debnath, S. Jiang, N. Strick, P. Haberfield and R. A. Neurath, *J. Med. Chem.*, 1994, **37**, 1099.

12 H. Arthanari, S. Basu, T. L. Kawano and P. H. Bolton, *Nucleic Acids Res.*, 1998, **26**, 3724.

13 (*a*) P. Bigey, S. H. Soennichsen, B. Meunier and P. E. Nielsen, *Bioconjugate Chem.*, 1997, **8**, 267; (*b*) B. Mestre, M. Pitie, C. Loup, C. Claparols, G. Pratviel and B. Meunier, *Nucleic Acids Res.*, 1997, **25**, 1022; (*c*) H. Li, O. S. Fedorova, W. R. Trumble, T. Fletcher and L. Czuchajowski, *Bioconjugate Chem.*, 1997, **8**, 49; (*d*) S. Mettath, B. R. Munson and R. K. Pandey, *Bioconjugate Chem.*, 1999, **10**, 94; (*e*) K. Berlin, R. K. Jain, M. D. Simon and C. Richert, *J. Org. Chem.*, 1998, **63**, 1527; (*f*) M. Tabata, A. K. Sarker and K. Watanabe, *Chem. Lett.*, 1998, 325.

14 (*a*) B. Meunier, *Chem. Rev.*, 1992, **92**, 1411; (*b*) W. Knapp Pogozelski and T. D. Tullius, *Chem. Rev.*, 1998, **98**, 1089.

15 C. J. Burrows and J. G. Muller, *Chem. Rev.*, 1998, **98**, 1109.

16 B. Armitage, *Chem. Rev.*, 1998, **98**, 1171.

17 E. Di Mauro, R. Saladino, P. Tagliatesta, V. De Sanctis and R. Negri, *J. Mol. Biol.*, 1998, **282**, 43.

18 N. Robic, C. Bied-Charreton, M. Perrée-Fauvet, C. Verchère-Béaur, L. Salmon, A. Gaudemer and R. F. Pasternack, *Tetrahedron Lett.*, 1990, **31**, 4739.

19 R. H. Jin, S. Aoki and K. Shima, *Chem. Commun.*, 1996, 1939.

20 (*a*) A. Salehi, H. Y. Mei and T. Briuce, *Tetrahedron Lett.*, 1991, **32**, 3453; (*b*) M. Perrée-Fauvet and N. Gresh, *Tetrahedron Lett.*, 1995, **36**, 4227.

21 Note. Our work on the synthesis, spectroscopic study of their interaction with DNA and possible bioapplication of onium porphyrins was presented at the XXI International Macrocyclic Conference, Montecatini, Italy, June 1996, abstracts p. 163. During preparation of the manuscript the work of a Japanese group[22] came to our attention. They use 4-chloromethylbenzaldehyde to synthesize porphyrin derivatives $\mathbf{P_3}$ and $\mathbf{P_4}$.

22 R. Jin, S. Aoki and K. Shima, *J. Chem. Soc.*, *Faraday Trans.*, 1997, **93**, 3945.

23 N. E. Mukundan, G. Petho, D. W. Dixon, M. S. Kim and L. G. Marzilli, *Inorg. Chem.*, 1994, **33**, 4676.

24 R. F. Pasternack, E. J. Gibs and J. J. Villafranca, *Biochemistry*, 1983, **22**, 2406.

25 F. J. Vergeldt, R. B. M. Koehorst, A. van Hoek and T. J. Schaafsma, *J. Phys. Chem.*, 1995, **99**, 4397.

26 I. E. Borisevitch and S. C. M. Gandini, *J. Photochem. Photobiol. B*, 1998, **43**, 112.

27 D. T. Croke, L. Perouault, M. A. Sari, J. P. Battioni, D. Mansuy, C. Helene and T. Le Doan, *J. Photochem. Photobiol. B.*, 1993, **18**, 41.

28 S. Schenken and S V. Jovanovich, *J. Am. Chem. Soc.*, 1997, **119**, 617.

29 F. Wilkinson, V. P. Helman and A. B. Ross, *J. Phys. Chem. Ref. Data*, 1995, **24**, 663.

30 F. Wilkinson, V. P. Helman and A. B. Ross, *J. Phys. Chem. Ref. Data*, 1993, **22**, 113.

31 B. C. Bookser and T. C. Bruice, *J. Am. Chem. Soc.*, 1991, **113**, 4208.

32 L. Wen, M. Li and J. B. Schlenoff, *J. Am. Chem. Soc.*, 1997, **119**, 7726.

33 R. R. Wells, J. E. Larson, R. C. Grant, B. E. Shortle and C. R. Cantor, *J. Mol. Biol.*, 1970, **54**, 465.

34 (*a*) P. Kubát, M. Jirsa and Z. Zelinger, *Radiat. Res.*, 1997, **148**, 382; (*b*) K. Lang, D. M. Wagnerová, P. Engst and P. Kubát, *J. Chem. Soc.*, *Faraday Trans. 2*, 1992, **88**, 677.

35 R. F. Pasternack, C. Bustamante, P. J. Collings, A. Giannetto and E. J. Gibs, *J. Am. Chem. Soc.*, 1993, **115**, 5393.

36 R. Jasua, D. M. Jameson, C. K. Nashijo and R. W. Larsen, *J. Phys. Chem. B*, 1997, **101**, 1444.

37 J. D. McGhee and P. H. von Hippel, *J. Mol. Biol.*, 1974, **86**, 469.

38 A. Cupane, M. Leone, L. Cordone, H. Gilch, W. Dreybrodt, E. Unger and R. Schweitzer-Stenner, *J. Phys. Chem.*, 1997, **100**, 14192.

39 K. Kalyasundaram, *Photochemistry of Polypyridine and Porphyrin Complexes*, Academic Press, London, 1992.

40 P. W. Bohn, *Annu. Rev. Phys. Chem.*, 1993, **44**, 37.

41 K. Kano, H. Minamizono, T. Kitae and S. Negi, *J. Phys. Chem. B*, 1997, **101**, 6118.

42 E. W. Knapp, *Chem. Phys.*, 1984, **85**, 73.

43 N. Maiti, S. Mazumdar and N. Periasamy, *J. Phys. Chem. B*, 1998, **102**, 1528.

44 O. Ohno, Y. Kaizu and H. Kobayashi, *J. Chem. Phys.*, 1993, **99**, 4128.

45 I. Carmichael and G. L. Hug, *J. Phys. Chem. Ref. Data*, 1986, **15**, 1.

46 R. F. Pasternack, E. J. Gibs, A. Gaudemer, A. Anteby, S. Bassner, L. De Poy, D. H. Turner, A. Williams, F. Laplace, M. H. Landsard, C. Merienne and M. Perée-Fauet, *J. Am. Chem. Soc.*, 1985, **107**, 8178.

47 R. Kuroda and H. Tanaka, *J. Chem. Soc.*, *Chem. Commun.*, 1994, 1575.

48 M. J. Carvlin and R. J. Fiel, *Nucleic Acid Res.*, 1983, **11**, 6121.

49 L. M. Fisher, R. Kuroda and T. T. Fakai, *Biochemistry*, 1985, **24**, 3199.

50 Ch. Schen and C. S. Foote, *J. Am. Chem. Soc.*, 1995, **117**, 6439.

51 Ch. Schen and C. S. Foote, *J. Am. Chem. Soc.*, 1993, **115**, 10446.

52 H. Kasai, Z. Yamazumi, M. Berger and J. Cadet, *J. Am. Chem. Soc.*, 1992, **114**, 9692.

Paper a909466k